Cooperative Protein–DNA Interactions: Effects of KCl on λ *c*I Binding to O_R[†]

Kenneth S. Koblan and Gary K. Ackers*

Department of Biochemistry and Molecular Biophysics, Washington University School of Medicine, St. Louis, Missouri 63110

Received February 7, 1991; Revised Manuscript Received May 24, 1991

ABSTRACT: The effects of monovalent salt activity on the site-specific and cooperative interactions of *c*I repressor with its three operator sites O_R were studied by using quantitative DNase I footprint titration methods. Individual-site binding isotherms were obtained for binding repressor dimers to each site of wild-type O_R and to mutant operator templates in which binding to one or two sites has been eliminated. The standard Gibbs energies for intrinsic binding, ΔG_1, ΔG_2, and ΔG_3, and cooperative interactions, ΔG_{12} and ΔG_{23}, were determined at each condition (range 50–200 mM KCl). It is found that the dimer affinity for each of the three sites increases as [KCl] decreases, a striking result given that the monomer–dimer equilibrium shifts toward monomer formation under identical solution conditions [Koblan, K. S., & Ackers, G. K. (1991) *Biochemistry* (preceding paper in this issue)]. The magnitudes of ion-linked effects are found to differ at the three operator sites, while the intrinsic interaction binding free energies for sites O_R1 and O_R3 change in parallel over the entire range of [KCl]. The KCl dependencies at O_R1 and O_R3 represent the average release of 3.7 ± 0.6 and 3.8 ± 0.6 apparent ions, respectively. By contrast, the KCl dependency of O_R2 binding corresponds to the displacement of 5.2 ± 0.7 apparent ions. The ability of *c*I repressor to discriminate between the three operator sites thus appears linked to ion binding/release reactions.

Control of transcriptional initiation often involves the interactions of regulatory proteins with specific DNA sequences. The combination of allosteric repressors, activators, and complex promoter elements generates a diverse array of mechanisms by which gene regulation is modulated. In many cases, the identified promoter elements have been found to interact with a group of structurally related proteins. Examples of these systems in prokaryotes include the phages λ and 434, while in eukaryotes the Jun/Fos and ATF/CREB families contain at least six different ligands in each group (Kouzarides & Ziff, 1989; Hai et al., 1989). A common feature which adds even more complexity is the finding that many regulatory proteins bind DNA as oligomers. In prokaryotes, many examples of homodimers exist (λ *c*I and *cro* repressors). In eukaryotes, the situation appears to be more complex. In the case of Jun protein, it can bind as a homodimer or as a Jun–Fos heterodimer (Chiu et al., 1989; Schutte et al., 1989).

A research program of this laboratory has been focused on detailed thermodynamic studies of the right operator region (O_R)[1] of bacteriophage λ (Ackers et al., 1982, 1983; Shea & Ackers, 1985; Brenowitz et al., 1986a,b, 1989; Senear et al., 1986; Senear & Ackers, 1990; Beckett et al., 1991). This system serves as a prototype for understanding multisite, multiprotein regulatory systems. Interactions of the phage-encoded homodimers, *c*I and *cro* repressors, with the three operator sites constitute the primary control switch between lysogenic and lytic phage development [see Ptashne (1986) for a review]. The footprint titration technique, a quantitative method for measuring individual-site thermodynamics (Brenowitz et al., 1986a,b), coupled with determination of dimerization constants (Beckett et al., 1991; Koblan & Ackers, 1991) resolves the energetically significant interactions of the system (Koblan et al., 1991). These interactions include intrinsic local-site binding and pairwise site–site cooperativity (Ackers et al., 1982; Senear & Ackers, 1990). The combination of thermodynamic information from this approach with recent crystallographic structures of the λ *c*I repressor–operator (Jordan & Pabo, 1988) may provide insights into the physicochemical basis for cooperativity and site specificity.

In the present study, we have employed the footprint titration method to determine the effects of monovalent salt ([KCl]) activity on *c*I repressor–O_R interactions. At each KCl concentration, the individual-site isotherms for wild-type O_R and three additional mutants were analyzed to resolve the Gibbs free energies for *c*I binding to each site along with the additional cooperative free energy terms. Salt effects were studied because of our expectation that the electrostatic potential around both the DNA and the *c*I dimers could significantly affect the energetics of both site-specific recognition and cooperative interactions, and because of the general importance of salt effects to the understanding of protein–DNA systems (Record et al., 1977, 1978; Lohman, 1985). Studies on the monomer–dimer equilibrium of *c*I repressor (Koblan & Ackers, 1991) support the idea that ions (and particularly cations) are important in stabilizing the dimer interface. Results of the present study indicate a significant contribution by counter/co-ion binding and release to the overall free energies of site-specific ligation. Over a range of conditions, it is found that differences in the intrinsic binding to each of the three sites are maintained while cooperative interactions between adjacently bound dimers are relatively insensitive to variations in [KCl]. The monomer–dimer equilibrium, however, is shifted by decreasing [KCl] toward monomers under these same solution conditions. These results suggest that the intersubunit contact between monomers within the dimer may be quite different from that between dimers bound adjacently on the DNA. The λ control system can regulate not only

[†] Supported by National Institutes of Health Grants GM39343 and R37-GM24486.

* Correspondence should be addressed to this author.

[1] Abbreviations: DNase I, bovine pancreas deoxyribonuclease I (EC 3.1.21.1); bis(acrylamide), *N*,*N*′-methylenebis(acrylamide); TEMED, *N*,*N*,*N*′,*N*′-tetramethylethylenediamine; BSA, bovine serum albumin; CT-DNA, calf thymus DNA; $NaDodSO_4$, sodium dodecyl sulfate; bp, base pair(s); O_R, λ right operator; Tris, tris(hydroxymethyl)aminomethane; Bistris, [bis(2-hydroxyethyl)amino]tris(hydroxymethyl)-methane.

0006-2960/91/0430-7822$02.50/0 © 1991 American Chemical Society

site-specific ligation but also the population of active dimeric species.

Materials and Methods

Chemical Reagents. α-^{32}P-Labeled deoxyribonucleotides (3000 Ci/mmol) were from Amersham; unlabeled deoxyribonucleotides were from P-L Biochemicals. Electrophoresis-grade acrylamide, bis(acrylamide), ammonium persulfate, and TEMED were Bio-Rad. Urea was sequential grade from Pierce Chemical Co. Acrylamide, bis(acrylamide), and urea were deionized with Bio-Rad AG501-X8 resin prior to use. CsCl was biochemical grade from Gallard–Schlesinger. All other reagents were reagent or analytical grade.

Biological Materials. Restriction endonucleases were from IBI or New England Biolabs. The large (Klenow) fragment of *Escherichia coli* DNA polymerase I and bovine serum albumin (BSA) (acetylated–nucleic acid enzyme grade) were from Bethesda Research Labs (BRL). Calf thymus DNA (CT-DNA) was from P-L Biochemicals. Bovine pancreas deoxyribonuclease I (DNase I, code D) from Worthington was stored as a 2 mg/mL stock solution in 150 mM NaCl/50% glycerol at −70 °C and diluted appropriately into assay buffer less BSA and CT-DNA, immediately prior to exposure. The relative catalytic activity of DNase I was determined at each [KCl] in order to obtain constant backbone nicking over the entire salt range.

The cI repressor protein used in these studies was purified according to the procedure previously described (Johnson et al., 1980). It is greater than 95% pure as judged by electrophoresis on $NaDodSO_4$ gels, but only 56% active, on the basis of stoichiometry experiments of the type described by Sauer (1979) and Johnson (1980), and based on $\epsilon^{280nm}_{mg/mL\text{-}cm} = 1.18$. Total active monomer concentrations were calculated from the stoichiometry experiments. The monomer–dimer equilibrium constant was determined at each condition studied (Koblan & Ackers, 1991).

Preparation of Operator DNA. Plasmids were purified by the procedure of Birnboim and Doly (1979) followed by CsCl density centrifugation (Maniatis et al., 1982). Plasmid pKB252 (Backman et al., 1976) containing the wild-type (O_R^+) λ operator was a gift from H. Nelson and R. Sauer. Reduced-valency mutant templates contain a single base pair substitution in one or two of the operator binding sites, which eliminate (−) site-specific repressor ligation. Plasmids which contained mutant operator regions, pBJ301 (O_R1^-), pBJ303 ($O_R1^-3^-$), pBJ306 (O_R2^-) (Meyer et al., 1980), and pAH19 (O_R3^-) (Maurer et al., 1980), were gifts from J. Eliason and M. Ptashne. Operator-containing fragments were excised from the plasmids with *Bgl*II (bp 38 103 in the λ *cro* gene) and either *Hin*dIII (bp 37 459) or *Pst*I (bp 37 001) in the λ cI gene, yielding fragments of 648 and 1102 bp, respectively. Preparation and radiolabeling of the restriction fragments were by standard procedures (Maniatis et al., 1982). The typical specific radioactivity of freshly labeled DNA [(7–10) × 10^6 Ci/mol] was used to estimate the operator concentration in binding experiments.

Individual-Site Binding Experiments. Experiments were conducted by using the quantitative DNase I footprint titration method, essentially as described previously (Brenowitz et al., 1986a). All equilibrium binding experiments were conducted in a buffer (assay buffer) consisting of 10 mM Bistris, 200, 150, 100, or 50 mM KCl, 2.5 mM $MgCl_2$, 1.0 mM $CaCl_2$, 100 μg/mL BSA, and 2 μg/mL CT-DNA (sonicated) at pH 7.00 ± 0.01 and 20 ± 0.01 °C. Reaction mixtures containing 15 000–25 000 cpm of ^{32}P-operator DNA (less than 10 pM in operator-containing fragments) in a volume of 200 μL were incubated for 1–2 h prior to DNase exposure. The [DNase I], 3–150 ng/mL (final), was varied to correct for the increased backbone nicking as the [KCl] decreased. All DNase exposures were conducted for 1.0 min prior to quenching. Electrophoresis on 8% acrylamide–urea gels and autoradiography were as described previously (Brenowitz et al., 1986a).

The optical density of the film is collected in two dimensions by an Eikonix 1412 CCD camera. Linearity of the camera was determined both before and after data collection by scanning a precalibrated step wedge (Kodak). The array of optical densities corresponding to 150-μm pixels on the autoradiogram is processed interactively with programs developed in this laboratory. Fractional occupancy of the operator sites is monitored by the ratio of the integrated optical density of a series of bands which correspond to a binding site to the optical density of a similar series of bands outside the binding site where no titration occurs (Brenowitz et al., 1986a).

Numerical Analysis. The footprint titration data were analyzed according to the appropriate binding functions by using nonlinear least-squares methods of parameter estimation. The fitting program (Johnson et al., 1976; Johnson & Frasier, 1985) uses a variation of the Gauss–Newton procedure (Hildebrand, 1956) in order to determine the best-fit model-dependent parameters which yield a minimum in the variance. The resolved variance ratio is predicted by an F statistic (Box, 1960) to determine the worst case joint confidence intervals for the fitted parameters. Confidence intervals (67%) correspond to approximately one standard deviation.

In order to resolve all of the highly correlated Gibbs free energy terms uniquely, it is necessary to combine results from experiments on an appropriate set of templates (Shea, 1983; Brenowitz et al., 1986a; Senear et al., 1986). In the simultaneous analysis of a composite data set from different experiments (wild type and mutant templates), weighting factors were employed to account for variations in experimental noise. To obtain appropriate weighting factors, each experiment was first analyzed independently to obtain the best "phenomenological" fit (Senear et al., 1986; Koblan et al., 1991). Combinations of cooperatively terms, ΔG_{ij}, were input as fixed parameters in these separate analyses for cases in which cooperative interactions occurred. Then ΔG_1, ΔG_2, ΔG_3, and the titration end points were fitted parameters (Brenowitz et al., 1986a). The resolved variances for the best combination of ΔG_{ij} terms were assumed to indicate the precision of that set of individual data points. Normalized weighting factors (Bevington, 1969) were calculated by

$$\sigma_{ij} = N_t(1/\sigma_j^2)/\sum_j(N_j/\sigma_j^2) \quad (1)$$

where σ_{ij} is the weight assigned to data point i of experiment j, σ_j^2 and N_j are the variance and number of data points for experiment j, respectively, and $N_t = \sum_j N_j$.

At 100, 150, and 200 mM KCl, the approximation that $[P]_{total} \approx [P]_{free}$ is accurate because the operator concentration is low relative to the equilibrium constants. The free dimer concentration is calculated directly from the truncated repressor conservation equation, $R_t = R_1 + 2R_2$ (monomer units), and knowledge of the dimer dissociation constant, $k_d = R_1^2/R_2$. At 50 mM KCl, the repressor–DNA equilibrium constant is large enough that bound repressor could not be ignored. In order to analyze the 50 mM KCl data set, the full conservation equation was employed as previously described (Senear & Ackers, 1990):

$$R_t = R_1 + 2R_2 + 2O_t\sum_{s,j} f_s \quad (2)$$

where R_1, R_2, and O_t refer to repressor monomer, repressor

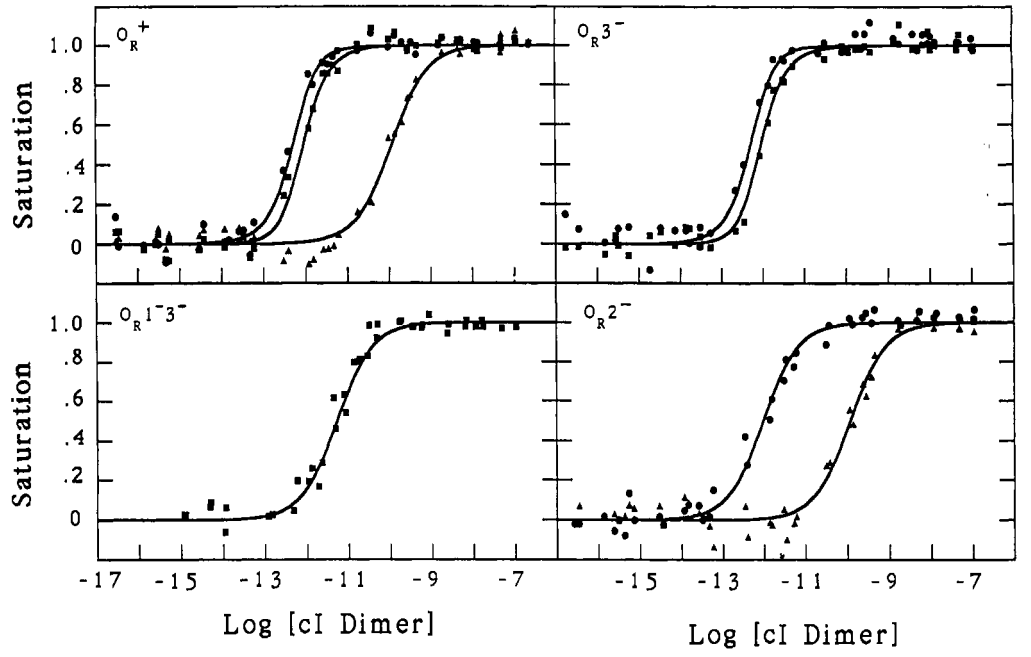

FIGURE 1: Individual-site binding of *c*I repressor to O_R^+, and to reduced-valency O_R mutants, at 50 mM KCl. Reaction conditions are pH 7, 20 °C, standard assay buffer. Panels show O_R^+, O_R3^-, $O_R1^-3^-$, and O_R2^- operators, respectively. (●) Site O_R1; (■) site O_R2; (▲) site O_R3. The solid curves represent the simultaneous analysis of the data in all panels by using the model described in Table I, and eq 4a–c. Estimated interaction free energies are given in Table II.

dimer, and operator concentration, respectively, and f_s is the probability of operator configuration s (Table I) with stoichiometry j. The f_s terms are defined by eq 4. The resolved ΔG_i and ΔG_{ij} values were not significantly affected by the uncertainty in estimating operator concentration.

Trapezoidal integration of the individual-site binding data was used to calculate the individual-site loading energies ($\Delta G_{1,i}$), which define the total free energy of binding at the given site, taking into account all the (shared) interactions (Ackers et al., 1983). The titration end points resolved by the best "phenomenological" fits were used in these calculations. All calculations were performed on a Hewlett-Packard 9000 computer system.

Results

Macromolecular Interaction Energies. Gibbs energy changes for both site-specific repressor binding and pairwise interactions are resolved by analyzing data using expressions which separately consider the individual sites. Binding expressions are constructed by considering the relative probability, f_s, of each operator configuration:

$$f_s = \frac{\exp(-\Delta G_s/RT)[R_2]^j}{\sum_s \exp(-\Delta G_s/RT)[R_2]^j} \quad (3)$$

ΔG_s is the sum of free energy contributions for configuration "s", R is the gas constant, T is the absolute temperature, $[R_2]$ is the concentration of free dimer, and j is the repressor stoichiometry in operator configuration "s". Interaction of *c*I dimers with the three operator sites yields nine possible configurations (Table I) (Shea, 1983). Five microscopic free energy terms can contribute to each species, ΔG_s.[2] Three intrinsic free energies, ΔG_1, ΔG_2, and ΔG_3, denote binding at a single site in the absence of binding at any others. The cooperative terms ΔG_{12} and ΔG_{23} refer to the excess free energy for binding to two sites simultaneously. By definition, ΔG_{ij} is the difference between the total free energy to fill the sites simultaneously (ΔG_T) and the sum of the intrinsic binding energies. The DNase I footprint titration technique resolves the fractional occupancies of each operator site, $\bar{Y}_i$, as a function of unbound $[R_2]$. The probabilities of the appropriate protein–DNA complexes (Table I) can then be summed to obtain the individual-site isotherms:

$$\bar{Y}_1 = f_2 + f_5 + f_6 + f_8 + f_9 \quad (4a)$$

$$\bar{Y}_2 = f_3 + f_5 + f_7 + f_8 + f_9 \quad (4b)$$

$$\bar{Y}_3 = f_4 + f_6 + f_7 + f_8 + f_9 \quad (4c)$$

Binding isotherms are obtained in an analogous manner for mutant operators where specific sites are not able repressor. For example, only configurations 1, 2, 4, and 6 (Table I) can exist for an O_R2^- mutant operator. It is assumed that interactions at any competent binding site are quantitatively unperturbed by the mutation (Johnson et al., 1979; Ackers et al., 1982).

Unique resolution of all interaction energies is not always possible for highly cooperative systems using binding data for the O_R^+ operator alone (Brenowitz et al., 1986a; Senear et al., 1986). In order to resolve the five microscopic interaction constants, binding experiments were conducted on O_R^+ and a set of reduced-valency mutants (Figures 1 and 2). Symbols represent individual data points while each curve represents an isotherm for one of the operator sites calculated by using the best resolved parameters from the simultaneous analysis. Results are given in Table II for all conditions. Data were analyzed simultaneously, by using the appropriate binding expressions in the form of eq 4a–c. At low-salt conditions (50–150 mM KCl), the templates employed were O_R^+, O_R2^-, O_R3^-, and $O_R1^-3^-$. Under these conditions, the mutation in the O_R1^- template, included in the 200 mM KCl data set, does reduce but *does not eliminate* site-specific recognition by the

[2] Previous quantitative analyses of *c*I repressor–O_R interactions have employed the statistical mechanical model presented by Ackers et al. (1982) which contained eight operator species. That model embodies features of cooperative coupling at O_R proposed by Johnson et al. (1979). In our analysis, we do not impose this "selection rule" which restricted cooperative interactions to sites O_R1 and O_R2 in the triply liganded operator. This gives rise to species 9 in Table I (Shea, 1983).

Table I: Microscopic Configurations and Associated Free Energy Contributions for the λ cI Repressor–Operator System, O_R[a]

species	operator configurations O_R1		O_R2		O_R3	free energy contributions
1	0		0		0	reference
2	R_2		0		0	ΔG_1
3	0		R_2		0	ΔG_2
4	0		0		R_2	ΔG_3
5	R_2	↔	R_2		0	$\Delta G_1 + \Delta G_2 + \Delta G_{12}$
6	R_2		0		R_2	$\Delta G_1 + \Delta G_3$
7	0		R_2	↔	R_2	$\Delta G_2 + \Delta G_3 + \Delta G_{23}$
8	R_2	↔	R_2		R_2	$\Delta G_1 + \Delta G_2 + \Delta G_3 + \Delta G_{12}$
9	R_2		R_2	↔	R_2	$\Delta G_1 + \Delta G_2 + \Delta G_3 + \Delta G_{23}$

[a] Individual operator sites are denoted by 0 if vacant or by R_2 if occupied by cI dimers. Cooperative interactions are denoted by (↔). ΔG_i (i = 1, 2, or 3) values are the intrinsic Gibbs free energies for binding to each of the three operator sites. ΔG_{ij} values are the free energies of cooperative interaction between liganded sites. Free energies are related to the corresponding microscopic equilibrium constants, k_i, by the relationship $\Delta G_i = -RT \ln k_i$.

repressor. Inability to determine how a site with a "reduced" affinity could cooperatively interact with adjacent sites leads us to simply exclude that data set from the analysis. Omission of data for that mutant ultimately manifests itself in the simultaneous analysis. Some of the parameters in eq 4a–c are highly correlated as a consequence of the cooperative coupling between the sites. Inclusion of reduced-valency mutants in the simultaneous analysis alters the combination of parameters in eq 4a–c. For this system, the O_R1^- data set is critical to any meaningful resolution of a ΔG_{23} term. Simulations indicate that inclusion of a "*real*" O_R1^- data set would allow resolution of the ΔG_{23} term and that the uncertainty in ΔG_{23} has no effect on the well-resolved intrinsic free energies or the cooperative free energy ΔG_{12}. Under all conditions where ΔG_{23} was unresolved in the model-dependent analysis, we have set it equal to the value of the ΔG_{12} term. The validity of this approach is supported by the fact that $\Delta G_{12} \approx \Delta G_{23}$ at all conditions studied to data (Brenowitz et al., 1986a; Senear & Ackers, 1990).

The steepness of the isotherms for O_R1 and O_R2 is a direct demonstration of the cooperative ligation at both sites (Figures 1 and 2). Analysis of individual O_R^+ experiments (each condition) always yielded a minimum variance for $\Delta G_{ij} < 0$. This trend leads to greater confidence in the cooperative nature of the binding than indicated by the confidence limits for individual experiments which could not exclude $\Delta G_{ij} = 0$ in every case. Previous studies in this laboratory have demonstrated an asymptotic limit to the shapes of isotherms for cooperatively coupled sites in this system (Senear et al., 1986). In the range 50–150 mM KCl, the data of the present study are very close to the asymptotic limit (calculations not shown).

Footprint Titration Analysis of cI Binding to O_R. Repressor binding as a function of [KCl] is shown in Figure 2. Each panel displays the self-consistent results from duplicate sets of four separate experiments (O_R^+, and three reduced-valency mutant templates) at each salt concentration. The symbols

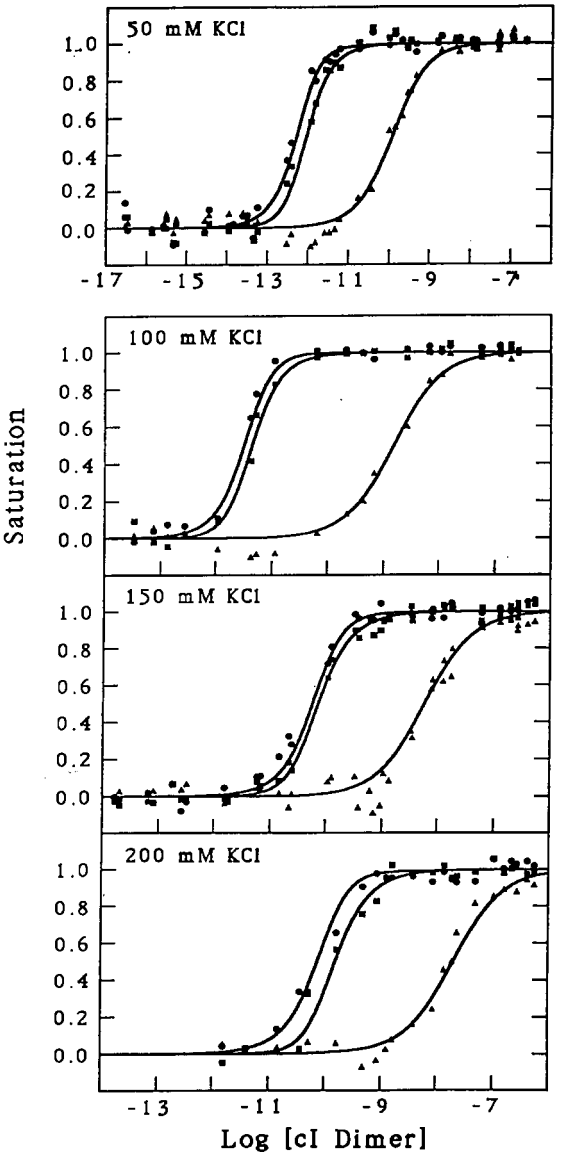

FIGURE 2: Cooperative binding of cI repressor to O_R versus [KCl]. Reaction conditions are pH 7, 20 °C, standard assay buffer plus increasing [KCl]. Panels (from top to bottom) are 50, 100, 150, and 200 mM KCl, respectively. Repressor dimer concentrations are calculated as described in the text. (●) Site O_R1; (■) site O_R2; (▲) site O_R3. The curves result from simultaneous analysis of data shown as well as data for reduced-valency mutants. The estimated Gibbs interaction energies are in Table II.

represent individual data points from binding experiments conducted on each template, while the solid curves represent the combined analysis of all DNA templates. The increase in affinity at each of the three sites as [KCl] decreases is clearly indicated by the leftward shifts in the positions of the curves. The repressor maintains high specificity for each site over the range studied as evidenced by lack of protection outside the operator sites (i.e., standard region). Preliminary

Table II: KCl Linkage of Microscopic Gibbs Energies of Repressor–O_R Interaction[a]

[KCl] (mM)	ΔG_1	ΔG_2	ΔG_3	ΔG_{12}	ΔG_{23}	s[c]
200	−13.2 ± 0.3	−10.7 ± 0.3	−10.2 ± 0.3	−3.0 ± 0.6	−3.0 ± 0.7	0.078
150	−13.5 ± 0.2	−12.2 ± 0.2	−10.9 ± 0.2	−1.8 ± 0.4	−1.8[b]	0.069
100	−14.7 ± 0.2	−13.2 ± 0.3	−11.8 ± 0.2	−2.7 ± 0.5	−2.7[b]	0.073
50	−16.1 ± 0.2	−15.1 ± 0.3	−13.3 ± 0.2	−1.4 ± 0.4	−1.4[b]	0.073

[a] Standard Gibbs energies (in kilocalories per mole ± 67% confidence intervals) of repressor–O_R interactions, obtained by simultaneous analysis of O_R^+ and reduced-valency mutant binding data. Reaction conditions were 20 °C, pH 7.00, plus [KCl] as noted. [b] Terms that were poorly resolved and therefore fixed. [c] Square root of the variance from simultaneous analysis.

experiments conducted from 1 to 10 mM KCl revealed that the repressor is in equilibrium with regions of the DNA outside the specific binding sites (O_R1, O_R2, and O_R3) in a concentration-dependent manner (data not shown). The simplest explanation for the observed effects is the presence of some enhanced "non-specific" DNA binding mode for *c*I repressor under low-salt conditions (1–10 mM KCl). Over the range 50–200 mM KCl, we were unable to detect any nonspecific binding to DNA regions outside of the specific sites (i.e., the ratio of specific to nonspecific affinities is at least 10^7).

The individual-site binding data were integrated numerically to determine the total Gibbs energy for saturating each site with ligand. This chemical work (Gibbs energy) to bind a mole of *c*I repressor at each respective site while stoichiometric amounts of ligand are also bound at the other sites is the *individual-site "loading" free energy* ($\Delta G_{l,i}$, Ackers et al., 1983). The loading free energy includes all energetic contributions that affect binding of a ligand at site *i*. These were evaluated in a model-independent manner according to

$$\Delta G_{l,i} = RT \ln \bar{X}_i = RT \int_0^1 \ln X \, dY_i \qquad (5)$$

where $\bar{X}_i$ is the median ligand activity [Wyman, 1964; see Ackers et al. (1983) for analysis in terms of individual sites] and Y_i is the fractional saturation at ligand activity X. In spite of the uncertainty in any model-dependent parameters, the individual-site loading free energies are precisely determined from the observed data points by using eq 5. The loading free energies provide a useful constraint on any model-dependent analysis in that the sum of the $\Delta G_{l,i}$'s is the total energy available to the system.

On the basis of 1 M total repressor standard state, the KCl-linked contributions to the individual-site loading free energies $\Delta\Delta G_{l,i}$ over the range are −3.4, −3.2, and −3.0 kcal/mol for O_R1, O_R2, and O_R3, respectively. The data in Figure 2 have been analyzed on the basis of repressor dimer concentrations dictated by our dissociation studies conducted under identical solution conditions (Kobalan & Ackers, 1991). The free energy of dimerization is itself a strong function of the [KCl] with dimers stabilized by 1.9 kcal/mol as the monovalent salt concentration increases (range 1–200 mM). Physical–chemical dissection of coupled protein–protein and protein–DNA interactions in this, and similar, systems must include quantitative measurement of the functionally relevant polymerization reactions.

Salt-Linked Effects. The effect of salt activity on the equilibrium constants is shown in Figure 3. The intrinsic binding energies are well resolved as indicated by the narrow confidence intervals (error bars, Figure 3) for these parameters. The repressor maintains its relative order of affinities, $O_R1 > O_R2 > O_R3$, over the range studied. Our results are in qualitative agreement with a previous report that increasing concentrations of salt reduce the stability of the *c*I repressor–operator complex (Ptashne, 1967). Evaluation of differences between the cooperative free energies is less certain due to the larger error in the ΔG_{12} term and lack of confidence in the ΔG_{23} term. No interpretable pattern is readily apparent for the KCl-linked effect on the cooperative term ΔG_{12}.

The KCl-linked effects on binding are in the same direction for the three sites and indicate that ligation is linked to overall ion release. The plots of ln K_i vs ln [KCl] are linear within experimental error for all three sites. It is important to recognize that in principle these plots should exhibit some curvature due to any anion release by the repressor upon binding to the DNA sites (deHaseth et al., 1977; Record et al., 1977, 1978), as well as any linkages to preferential interactions or

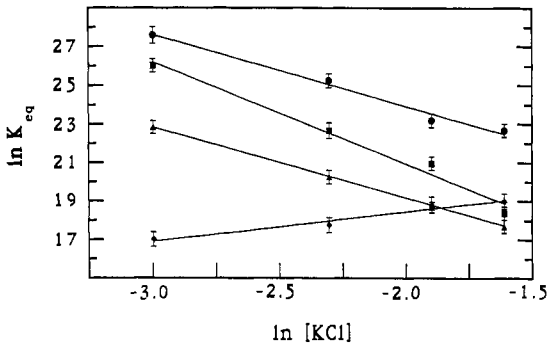

FIGURE 3: KCl-linked effects on the free energies of *c*I repressor–O_R interactions at pH 7, 20 °C. Gibbs energies corresponding to microscopic interaction parameters for site-specific binding, ΔG_1 (●), ΔG_2 (■), and ΔG_3 (▲), resolved by simultaneous analysis of individual-site binding data as in Figure 1 and *c*I dimerization, ΔG_D (♦) [see Koblan and Ackers (1991)], are plotted. Error bars present 67% confidence intervals corresponding to approximately one standard deviation.

binding by the divalent cations Mg^{2+} and Ca^{2+} [see also Lohman (1985)]. A standard expression applicable at low to moderate salt concentrations is

$$\left(\frac{\partial \ln K_{eq}}{\partial \ln [KCl]}\right)_{Mg^{2+},Ca^{2+}} = \Delta n_{K^+} + \Delta n_{Cl^-} \qquad (6)$$

where Δn_{K^+} and Δn_{Cl^-} are preferential interaction terms for the monovalent cations and anions, respectively, at constant chemical potentials of protons and divalent cations. Release of anions by the repressor upon binding to the DNA may introduce curvature into the plot of ln K_{eq} vs ln [KCl] even at constant pH and divalent ion concentrations, by providing an an additional source of variation for the Δn_{Cl^-} term. Since the range of salt concentrations in the present study is narrow, the data do not rule out all possible curvature. The combined effects of salts with different valencies will also produce nonlinear plots of ln K_{eq} vs ln [KCl]. A strategy for elucidating these effects through experiments with mixed-composition salts has been discussed by Lohman (1985).

While the uncertainties discussed above impose limitations on exact mechanistic interpretations, the differences in the slopes of the curves in Figure 3 nevertheless indicate a significant difference in KCl-linked effects at O_R1 and O_R3 compared to O_R2. At O_R1 and O_R3, approximately 3.7 ± 0.6 apparent ions are displaced while at O_R2 5.2 ± 0.7 apparent ions are involved. These slopes represent the average release of K^+ and Cl^- and do not include any displacement of divalent cations which may also be occurring. Formation of the interface internal to the dimer may involve the absorption of approximately 1.5 mol of ions (Koblan & Ackers, 1991).

Discussion

In this study, we have used quantitative footprint titration to measure the effects of monovalent salt on interactions of the λ *c*I repressor and O_R. Simultaneous analysis of individual-site isotherms for wild type and several reduced-valency mutant operators (Senear et al., 1986) allows us to resolve effects on site-specific recognition and cooperative interactions between adjacently bound repressors. Independent measurement of the thermodynamics of repressor dimerization under identical solution conditions (Koblan & Ackers, 1991) allows us to separate the roles that ions play in these coupled protein–protein and protein–DNA assembly reactions.

Salt Effects on Repressor Binding. The Gibbs energies detailed in Table II demonstrate two fundamental results. First, the site-specific binding of repressor to the three right

operators is sensitive to the concentration of monovalent salt. This salt dependence is different among the three sites, indicating fundamental differences in ionization reactions. Second, there is essentially no effect of [KCl] on the cooperative interactions.

At all three operators, repressor binding is apparently linked to ion release. The parallel between sites O_R1 and O_R3 versus O_R2 is quite striking and reminiscent of results obtained in the previous study from this laboratory (Senear & Ackers, 1990) on cI binding to O_R as a function of pH. The effect of protons on O_R1 and O_R3 binding (pH 6–7 range) was found to change in parallel while site-specific binding to O_R2 was quite different [Table III of Senear and Ackers (1990)]. The near-constancy of cooperative interactions is also common to both studies. It is compelling to speculate that both sets of results (pH and [KCl]) point to a common motif by which sites O_R1 and O_R3 are recognized and specifically ligated.

Assignment of Effects. The recent crystallographic study on the cI repressor NH_2-terminal domain/O_L1 indicates that the complex is stabilized by a network of hydrogen bonds between the protein and bases in the major groove along with phosphate oxygens of the DNA (Jordan & Pabo, 1988). Specific contacts between the protein and base pairs in the operator regions occur at position 2 (A·T), and positions 4 and 6 (both G·C), in each operator half-site. These base pair positions are strictly conserved in all but one of the half-sites which make up both O_R and the left operator region, O_L. It appears that these contacts may play crucial roles in the discrimination between specific and nonoperator DNA. Our observation that approximately 3.7 ions are released upon O_R1 and O_R3 binding and 5.2 ions upon O_R2 binding is consistent with the small number of charged residues which actually interact with phosphates (Jordan & Pabo, 1988).

Interpretation of the parallel between site O_R1 and O_R3 binding as a function of [KCl] and proton activity lead us to consider the specific DNA sequences themselves. Site-specific recognition and binding interactions which occur with high affinity (i.e., −10 to −15 kcal/mol) clearly represent complex processes that are not presently understood in any system. Patterns obtained by driving the system with different thermodynamic potentials must correlate at some level with specific structures accessible to the system. Given the results of this study and the previous one from this laboratory (Senear & Ackers, 1990), it appears that ligation of O_R1 and O_R3 may involve similar ionic equilibria at the level of both the protein and the DNA. Clearly, the situation is more complex since cI–O_R1 and cI–O_R3 are not iso-energetic structures.

References

Ackers, G. K., Johnson, A. D., & Shea, M. A. (1982) *Proc. Natl. Acad. Sci. U.S.A. 79*, 1849–1853.

Ackers, G. K., Shea, M. A., & Smith, F. N. (1983) *J. Mol. Biol. 170*, 223–242.

Backman, K., Ptashne, M., & Gilbert, W. (1976) *Proc. Natl. Acad. Sci. U.S.A. 73*, 4174–4178.

Beckett, D., Koblan, K. S., & Ackers, G. K. (1991) *Anal. Biochem.* (in press).

Bevington, P. R. (1969) *Data Reduction and Error Analysis for the Physical Sciences*, McGraw-Hill, New York.

Birnboim, H., & Doly, J. (1979) *Nucleic Acids Res. 7*, 1513–1523.

Box, G. D. P. (1960) *Ann. N.Y. Acad. Sci. 86*, 792.

Brenowitz, M., Senear, D. F., Shea, M. A., & Ackers, G. K. (1986a) *Proc. Natl. Acad. Sci. U.S.A. 83*, 8462–8466.

Brenowitz, M., Senear, D. F., Shea, M. A., & Ackers, G. K. (1986b) *Methods Enzymol. 130*, 132–181.

Brenowitz, M., Senear, D. F., & Ackers, G. K. (1989) *Nucleic Acids Res. 17*, 3747–3755.

Chadwick, P., Pirrotta, V., Steinberg, R., Hopkins, N., & Ptashne, M. (1970) *Cold Spring Harbor Symp. Quant. Biol. 35*, 283–294.

Chiu, R., Angel, P., & Karin, M. (1989) *Cell 59*, 979–986.

deHaseth, P. L., Lohman, T. M., & Record, M. T., Jr. (1977) *Biochemistry 16*, 4783–4790.

Hai, T., Liu, F., Coukos, W. J., & Green, M. R. (1989) *Genes Dev. 3*, 2083–2090.

Hildebrand, F. B. (1956) *Introduction to Numerical Analysis*, McGraw-Hill, New York.

Johnson, A. (1980) Ph.D. Dissertation, Harvard University, Cambridge, MA.

Johnson, M. L., & Frasier, S. G. (1985) *Methods Enzymol. 117*, 301–342.

Johnson, M., Halvorson, H., & Ackers, G. K. (1976) *Biochemistry 15*, 5363–5367.

Johnson, A. D., Meyer, B. J., & Ptashne, M. (1979) *Proc. Natl. Acad. Sci. U.S.A. 76*, 5061–5065.

Johnson, A., Pabo, C., & Sauer, R. T. (1980) *Methods Enzymol. 65*, 839–856.

Jordan, S. R., & Pabo, C. O. (1988) *Science 242*, 893–899.

Koblan, K. S., & Ackers, G. K. (1991) *Biochemistry* (preceding paper in this issue).

Koblan, K. S., Bain, D. L., Shea, M. A., & Ackers, G. K. (1991) *Methods Enzymol.* (in press).

Kouzarides, T., & Ziff, E. (1989) *Cancer Cells 1*, 71–76.

Lohman, T. M. (1985) *CRC Crit. Rev. Biochem. 19*, 191–245.

Maniatis, T., Fritsch, E. F., & Sambrook, J. (1982) *Molecular Cloning—A Laboratory Manual*, Cold Spring Harbor Laboratory, Cold Spring Harbor, NY.

Maurer, R., Meyer, B. J., & Ptashne, M. (1980) *J. Mol. Biol. 138*, 147–161.

Meyer, B. J., Maurer, R., & Ptashne, M. (1980) *J. Mol. Biol. 139*, 163–194.

Ptashne, M. (1967) *Nature 214*, 232–234.

Ptashne, M. (1986) *The Genetic Switch*, Cell Press, Cambridge, MA.

Record, M. T., Jr., deHaseth, P. L., & Lohman, T. M. (1977) *Biochemistry 16*, 4791–4796.

Record, M. T., Jr., Anderson, C. F., & Lohman, T. M. (1978) *Q. Rev. Biophys. 11*, 103–178.

Sauer, R. (1979) Ph.D. Dissertation, Harvard University, Cambridge, MA.

Schutte, J., Viallet, J., Nau, M., Segal, S., Fedorko, J., & Minna, J. (1989) *Cell 59*, 987–997.

Senear, D. F., & Ackers, G. K. (1990) *Biochemistry 29*, 6568–6577.

Senear, D. F., Brenowitz, M., Shea, M. A., & Ackers, G. K. (1986) *Biochemistry 25*, 7344–7354.

Shea, M. A. (1983) Ph.D. Dissertation, Johns Hopkins University, Baltimore, MD.

Shea, M. A., & Ackers, G. K. (1985) *J. Mol. Biol. 181*, 211–230.

Wyman, J., Jr. (1964) *Adv. Protein Chem. 19*, 224–394.